

# Contribution of upregulated dipeptidyl peptidase 9 (DPP9) in promoting tumorigenicity, metastasis and the prediction of poor prognosis in non-small cell lung cancer (NSCLC)

Zhiyuan Tang<sup>1</sup>, Jun Li<sup>1</sup>, Qin Shen<sup>1</sup>, Jian Feng<sup>1</sup>, Hua Liu<sup>1</sup>, Wei Wang<sup>2</sup>, Liqin Xu<sup>1</sup>, Guanglin Shi<sup>1</sup>, Xumei Ye<sup>1</sup>, Min Ge<sup>1</sup>, Xiaoyu Zhou<sup>1</sup> and Songshi Ni<sup>1</sup>

<sup>1</sup>Department of Respiratory Medicine, Affiliated Hospital of Nantong University, Nantong 226001, Jiangsu, China

<sup>2</sup>Department of Pathology, Affiliated Hospital of Nantong University, Nantong 226001, Jiangsu, China

Dipeptidyl peptidase 9 (DPP9) is encoded by DPP9, which belongs to the DPP4 gene family. Proteins encoded by these genes have unique peptidase and extra-enzymatic functions that have been linked to various diseases including cancers. Here, we describe the expression pattern and biological function of DPP9 in non-small-cell lung cancer (NSCLC). The repression of DPP9 expression by small interfering RNA inhibited cell proliferation, migration, and invasion. Moreover, we explored the role of DPP9 in regulating epithelial-mesenchymal transition (EMT). The epithelial markers E-cadherin and MUC1 were significantly increased, while mesenchymal markers vimentin and S100A4 were markedly decreased in DPP9 knockdown cells. The downregulation of DPP9 in the NSCLC cells induced the expression of apoptosis-associated proteins both *in vitro* and *in vivo*. We investigated the protein expression levels of DPP9 by tissue microarray immunohistochemical assay (TMA-IHC) ( $n = 217$ ). Further we found mRNA expression levels of DPP9 in 30 pairs of clinical NSCLC tissues were significantly lower than in the adjacent non-cancerous tissues. Survival analysis showed that the overexpression of DPP9 was a significant independent factor for poor 5-year overall survival in patients with NSCLC ( $p = 0.003$ ). Taken together, DPP9 expression correlates with poor overall survival in NSCLC.

Lung cancer remains the leading cause of cancer-related mortality worldwide.<sup>1</sup> The two main types of lung cancer are small-cell lung cancer and non-small-cell lung cancer

**Key words:** DPP9, NSCLC, metastasis, apoptosis, prognosis

**Abbreviations:** ATCC: American Type Culture Collection; CI: confidence interval; DPP9: dipeptidyl peptidase 9; EMT: epithelial-mesenchymal transition; ECL: enhanced chemiluminescence; FBS: fetal bovine serum; HR: hazard ratio; IHC: immunohistochemical; NSCLC: non-small-cell lung cancer; OS: overall survival; SD: standard deviation; TMA: tissue microarray; TNM: tumor node metastasis

Additional Supporting Information may be found in the online version of this article.

This is an open access article under the terms of the Creative Commons Attribution-NonCommercial-NoDerivs License, which permits use and distribution in any medium, provided the original work is properly cited, the use is non-commercial and no modifications or adaptations are made.

**DOI:** 10.1002/ijc.30571

**History:** Received 29 June 2016; Accepted 30 Nov 2016; Online 10 Dec 2016

**Correspondence to:** Songshi Ni, Department of Respiratory Medicine, Affiliated Hospital of Nantong, University, Nantong, Jiangsu 226001, China, Tel.: +86-13706293196, Fax: +86-513-85519820, E-mail: jsntnss@163.com or Xiaoyu Zhou, Department of Respiratory Medicine, Affiliated Hospital of Nantong, University, Nantong, Jiangsu 226001, China, Tel.: +86-13706293196, Fax: +86-513-85519820, E-mail: hx730303@163.com

(NSCLC), with the latter accounting for approximately 85% of total Lung cancer diagnoses.<sup>2,3</sup> In recent years, despite the great progress that has been made in diagnosis and combined treatments including surgical resection, chemotherapy, radiation therapy, and targeted biological agents,<sup>4</sup> the overall prognosis of NSCLC patients remains poor, with a 5-year survival rate of approximately 15%.<sup>5</sup> Therefore, more intensive efforts should be made to investigate the initiation and progression of NSCLC. The development of NSCLC involves multiple genetic and epigenetic changes that contribute to the transformation of normal cells into cancer cells. Dipeptidyl peptidase 9 (DPP9) is a member of a family of ubiquitous atypical serine proteases,<sup>6</sup> which mediate diverse physiological and pathological processes beyond incretin degradation, such as cell migration, tumor cell invasion, and metastasis.<sup>7-9</sup> For example, the upregulation of DPP9 in human embryonic kidney (HEK293T) cells led to impaired cell adhesion and migration, as well as the enhancement of induced and spontaneous apoptosis.<sup>10</sup> Emerging evidence has also revealed that disordered DPP9 expression may play a crucial role in cancer initiation and progression. For example, the mRNA expression of DPP9 is significantly elevated in testicular cancer,<sup>11</sup> while DPP9 enzymatic activity is positively associated with tumor grade severity in human astrocytic tumors. Alterations in dipeptidyl peptidase-IV (DPP4) enzymatic activity are characteristic of malignant transformation. Through its well-characterized functionality in regulating the activity of bioactive peptides by removal of the N-terminal dipeptide, DPP-IV activity may

**What's new?**

Non-small-cell lung cancer (NSCLC) is associated with multiple genetic and epigenetic changes. Nonetheless, mechanisms underlying its initiation and progression are not well understood. The present study identifies a role for dipeptidyl peptidase 9 (DPP9), a DPP4 family member with suspected influence on tumor initiation and metastasis. In lung cancer cells *in vitro*, DPP9 repression inhibited cell proliferation, migration, and invasion, while its repression *in vivo* dramatically slowed tumor growth, greatly reducing tumor volume in DPP9 knockdown mice. In clinical NSCLC specimens, DPP9 upregulation was significantly associated with advanced TNM stage and was negatively prognostic for overall survival.

have profound effects upon metastatic potential and cell growth.<sup>12,13</sup> The inhibition of DPP8/9 in tumor cells decreased the number of viable cells because of a decreased cleavage of pro-apoptotic NPY,<sup>14</sup> also their activity has been found in human monocytes and U937 cells.<sup>15</sup> DPP8 and 9 are abundantly present in macrophage-rich regions of atherosclerotic plaques. Furthermore, DPP9 is upregulated after *in vitro* monocyte-to-macrophage differentiation. Moreover, inhibition or RNA silencing of DPP9 attenuates pro-inflammatory M1, but not M2, macrophage activation.<sup>16</sup> However, the expression pattern and biological functions of DPP9 in NSCLC remain to be elucidated. In the current study, we explored the roles and mechanisms of DPP9 in NSCLC progression. We showed that the repression of DPP9 inhibits proliferation, migration, and invasion in NSCLC cells. We also identified the overexpression of DPP9 as a significant poor prognostic factor for 5-year overall survival (OS) in patients with NSCLC, and found that DPP9 expression was significantly increased in NSCLC tissues compared with adjacent non-tumor tissues, and correlated with a poor OS rate in NSCLC patients.

**Material and Methods****Patients' clinical information and tissue samples**

This study included 217 NSCLC patients. A total of 217 cancerous tissues and 122 matched adjacent normal tissues were formalin-fixed and paraffin-embedded. Among this, 30 patients were consented and enrolled before surgery. We collected and frozen 30 pairs of matched tumorous and normal tissue samples. The ages of patients ranged from 37 to 83 years, with a median of 63.2 years, including 53 women and 164 men. We obtained the clinical characteristics from patients' medical records. None of the patients had received radiotherapy, neo-adjuvant chemotherapy or immunotherapy before surgery. All the samples were obtained from the human clinical biobank in Affiliated Hospital of Nantong University, Jiangsu Province, China.

**Cell lines and cell culture**

The human NSCLC cell lines A549, NCI-H1299, NCI-H1675 and NCI-H1650 were obtained from the Cell Bank, Type Culture Collection, Chinese Academy of Science (CBTCCAS, Shanghai, China). These cell lines were maintained in RPMI 1640 supplemented with 10% fetal bovine serum (FBS), 2 mM L-glutamine, 100 U/ml penicillin/streptomycin mixtures under a humidified atmosphere of 5% CO<sub>2</sub> at 37°C.

**RNA extraction and real-time PCR (RT-PCR)**

Total RNA was extracted with RNAiso Plus (TaKaRa, Japan) and reverse transcribed into cDNA using the PrimeScript RT Reagent Kit (TaKaRa, Japan) following the supplier's instructions. RT-PCR was performed using an ABI 7500 FAST Real-Time PCR System (Applied Biosystems, Carlsbad) and a SYBR Green Master Mix (Takara, Dalian, China). The levels of expressed genes were quantified with the 2<sup>-ΔΔCt</sup> method after normalizing to an endogenous reference GAPDH. The experiment was performed in triplicate. The following primers were used for PCR amplification: DPP9 forward: 5'-GTGGACCTGGAGACTCTC-3', DPP9 reverse: 5'-TTCCTC TTGGAGAAGATCAG-3'; GAPDH forward: 5'-GGTAGACA AGTTTCCCTT-3', GAPDH reverse: 5'-ATATGTTCTGGAT GATTCT-3'.

**Western blot analysis**

Briefly, cells were lysed in RIPA lysis buffer (P0013B, Beyotime Institute of Biotechnology, Nantong, China) at 48 hr following transfection as described below and protein concentration was determined by the BSA method (Beyotime Institute of Biotechnology). Equivalent quantities of protein were separated on a 10% SDS-polyacrylamide gels and then transferred to Polyvinylidene Fluoride (PVDF) Membrane. Membranes were blocked using 5% non-fat milk and incubated overnight with the appropriate primary antibody. The next day, they were washed three times with TBST and incubated with a HRP-conjugated secondary antibody (Beyotime Institute of Biotechnology) at 1:5,000 dilution for 1 hr at room temperature. Protein detection was performed using the enhanced chemiluminescence (ECL) system (Millipore, Bedford, MA). Primary immunoblotting antibodies were: anti-β-Actin(dilution 1:1,000, 4,970, Cell Signaling Technology, Danvers, MA), anti-DPP9(dilution 1:1,000, ab42080, Abcam, Cambridge, MA), anti-p53 (Epitomics, Burlingame, CA), anti-BAX(dilution 1:1,000, ab32503, Abcam), anti-APAF1(dilution 1:1,000, ab32372, Abcam), anti-MUC1(dilution 1:1,000, ab45167, Abcam), anti-S100A4(dilution 1:1,000, ab124805, Abcam), anti-E-cadherin(1:50, ab1416), anti-vimentin (1:1,000, ab92547, Abcam).

**Reagents, transfection and stable cell lines generation**

Four small interfering RNA targeting human DPP9 mRNA (named shDPP9, shRNA-1 sense: shRNA-1:5'-CCCTATG AAACCGCTGGAAAT-3'; shRNA-2 sense: 5'-GCTGCACTT

TCTACAGGAATA-3'; shRNA-3 sense: 5'-CCCAACGAGAG ACACAGTATT-3'; shRNA-4 sense: 5'-GCTGGTGAATAACT CCTTCAA-3') and the negative control duplex (named shControl, sense: 5'-TTCTCCGAACGTGTCACGT-3') with no significant sequence homology with any known gene were used for lose-of-function studies. The RNA duplexes were chemically synthesized by Biomics Biotech, Nantong, China. Oligonucleotide transfection was conducted using Lipofectamine 2000 reagents (Invitrogen) according to the manufacturer's protocol.

Amongst the most efficient sequences we selected shRNA-1 by RT-PCR and western blot analysis, and further continued with shRNA-1 alone. shRNA-1 sequence was binded with pGPH1/GFP/NEO vector. We cloned the full-length DPP9 cDNA into pCMV6/AC/GFP vector. All the cell lines with plasmids were screened by GFP testing. Then cells were cultured in the medium, which containing 200 µg/ml G418 (Invitrogen). The expressions of the plasmids were proved by RT-PCR. We isolated and further replicated cell clones after 30 days. Stable cell lines in which DPP9 was silenced were generated and named A549 shDPP9 and H1299 shDPP9. The corresponding controls were named A549 shControl and H1299 shControl.

#### Cell growth/cell viability assay

After seeding the A549, H1299, H1975 or H1650 cells into 96-well plates with approximately  $5 \times 10^3$  cells per well for 24 hr, the cells were transfected with the RNA duplex (shDPP9 or shControl) for up to 4 days at a final concentration of 50 nM. At each time point, the medium was removed and replaced with WST-8/CCK-8 (Dojindo Laboratories, Japan). After 1 hr of incubation at 37°C, the absorbance was measured in the spectrophotometer at 450 nm with a MRX II absorbance reader (Dy nex Technologies).

#### Cell migration and invasion assay

The cell migration and invasion assay was performed with transwell chambers (Millipore). For the invasion assay, the inserts were precoated on the upper-surface with Matrigel (BD Biosciences). After transfection, cells from different groups ( $8 \times 10^4$ ) were suspended in serum-free medium (0.2 ml) and added to the upper compartment. Then, 0.6 ml RPMI-1640 with 10% FBS was added to the lower compartment as a chemoattractant. After 24 hr of incubation at 37°C, the cells on the upper surface of the membrane were gently removed using a cotton swab, and cells on the lower surface of the membrane were fixed with 100% methanol and stained with 0.3% crystal violet. To quantify the degree of invasion and migration, five visual fields (total magnification,  $\times 200$ ) were randomly selected for each insert and counted under a light microscope (Olympus, Japan).

#### Immunohistochemical (IHC) staining

Two individuals assessed and marked the IHC staining independently. They were blinded to each other's scores and clinical characteristics of the samples. This tissue microarrays

(TMA) was generated by the manual Tissue Microarray System Quick-Ray (UT06, UNITMA, Korea). Core tissue samples (diameter of 2 mm) were obtained from paraffin embedded tissue sections and deposited in paraffin-recipient blocks. Paraffin tissue sections were dewaxed and rehydrated. For antigen retrieval, slides were heated in sodium citrate buffer (10 mM, pH 6.0) for 3 min. After blocking with Bovine Serum Albumin (BSA, Sigma, St. Louis, MO), the slides were incubated with anti-DPP9 (1:100, Abcam, Cambridge, MA) overnight at 4°C. The slides were washed three times with PBS and incubated with a HRP-conjugated secondary antibody for 1 hr at room temperature. A DAB solution was used for immunohistochemical staining. For the semi-quantification of positive strength, both the intensity (0, 1, 2, 3) and proportion of positive cells (0 to 100) were noted. Thus, the score range is from 0 (none was stained) to 300 (all was strongly stained). Then the X-file software (Rimm Laboratory at Yale University; <http://www.tissuearray.org/rimmlab>)<sup>17</sup> was applied to divide the protein expression into two categories (low expression and high expression) here, the High expression is from 80 to 300 microscopic score and Low expression is from 0 to 80 microscopic score, which were obtained from the microscopic IHC staining score of tumor cells collected from the patients.

#### In vivo tumorigenicity assays

Animal study was performed in accordance with the institutional guidelines for the care and use of animals. Male BALB/c-nude mice (4 weeks of age) were purchased from the Shanghai Experimental Animal Center, Chinese Academy of Sciences, Shanghai, China. A549 shControl, A549 shDPP9, H1299 shControl, H1299 shDPP9 cells ( $1 \times 10^7$  in 100 µl PBS) were injected subcutaneously into the right flank of each nude mouse. After palpable tumors had formed, two perpendicular diameters were measured using caliper every 3 days, and we used the formula  $V = (\text{width}^2 \times \text{length} \times 0.52)$  to calculate the tumor volume. We fixed part of the tumors in 10% formalin and subjected to the IHC staining and examination by pathology staff who has little information on the tumor status. The other parts of the tumors were frozen at  $-80^\circ\text{C}$  for our next experiments.

#### Statistical analysis

The data were expressed as the mean  $\pm$  standard deviation (SD). The significance of a difference between groups was tested using the  $\chi^2$  test for the clinical data of patients and two-sided *t* test for the data of cell experiments. OS rates were calculated using Kaplan-Meier method with log-rank test. Multivariate analysis by Cox regression analysis (proportional hazards model) was also performed for the prognostic factors. All analyses were completed with SPSS16.0 software (IBM) and a value of  $p < 0.05$  was considered statistically significant.

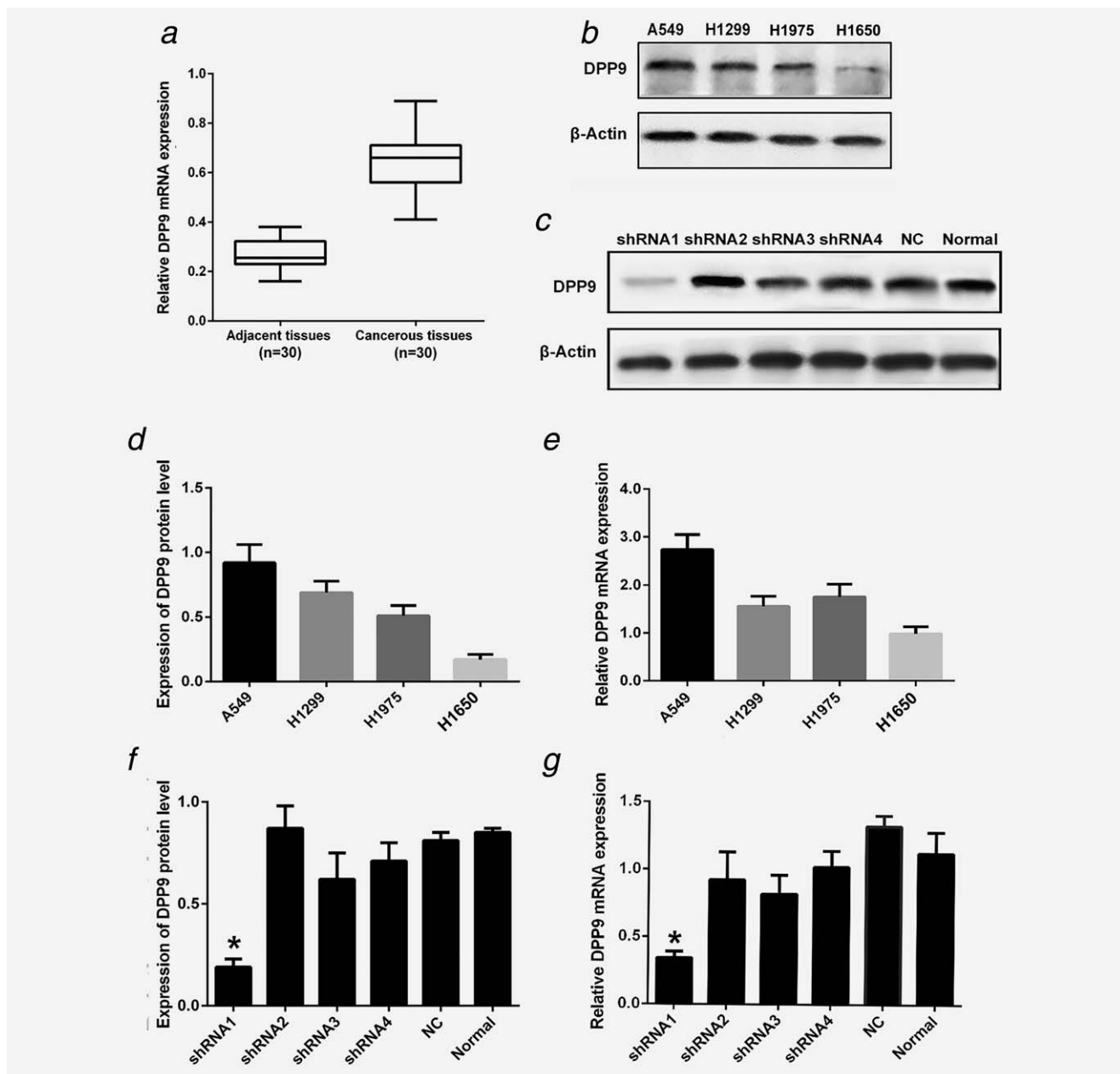


**Figure 1.** The expression of DPP9 in NSCLC tissues and cell lines. (a) The relative expression levels of DPP9 in individual 30 pairs of NSCLC tissues; (b and d) The protein expression of DPP9 in four NSCLC cell lines A549, H1299, H1975 and H1650; (e) The mRNA expression of DPP9 in four NSCLC cell lines; (c and f) Western blot analysis to select the most efficient shRNA in shDPP9-transfected cells; (g) The mRNA expression of four small interfering RNA in shDPP9-transfected cells compared with control and normal cells.

## Results

### DPP9 expression in NSCLC tissues and cell lines

To evaluate the expression of DPP9 in NSCLC, RT-PCR was performed in 30 pairs of clinical NSCLC tissues and adjacent non-cancerous tissues. DPP9 expression levels were significantly lower in tumor tissues than in non-tumor tissues ( $n = 30$ ) (Fig. 1a). We next examined DPP9 mRNA and protein expression in four NSCLC lines (A549, H1299, H1975 and H1650). As shown in Figures 1b, 1d and 1e, the highest DPP9 expression was detected in A549 cells, followed by H1299, H1975 and H1650,

both at the protein and mRNA level. A549 cells were transfected with four types of shDPP9 (shRNA-1, shRNA-2, shRNA-3 and shRNA-4) and negative control shRNA. Western blot analysis revealed reduced DPP9 protein expression (Fold change: 0.17 vs. 0.86, shRNA-1 vs. shControl) in shDPP9-transfected cells (Figs. 1c and 1f). A decrease in the mRNA expression (Fold change: 0.26 vs. 1.33, shRNA-1 vs. shControl) of DPP9 was also observed in shDPP9-transfected NSCLC cells (Fig. 1g). However, shRNA-1 had the highest silencing efficiency, so was used in the following loss-of-function experiments.

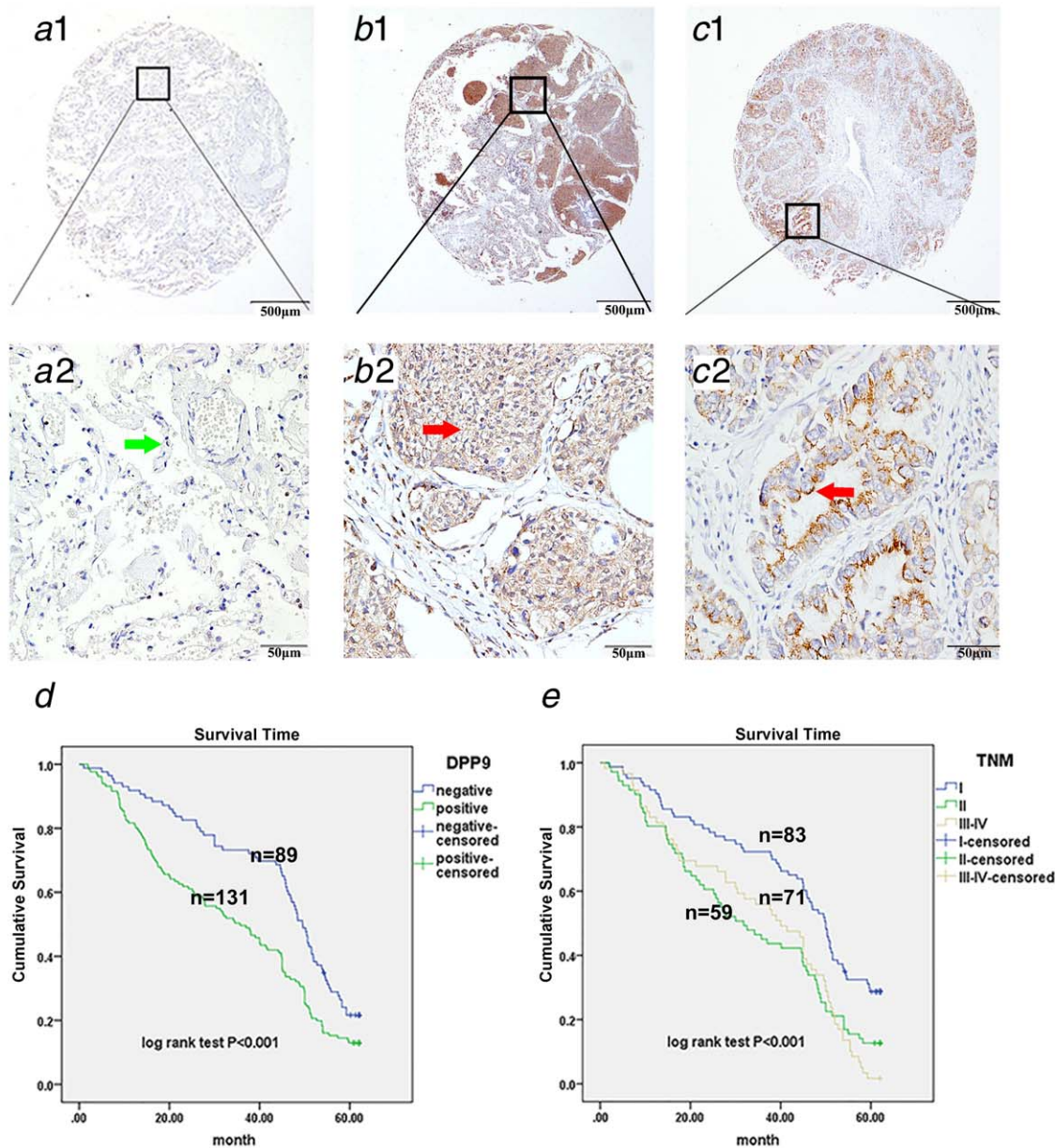


**Figure 2.** DPP9 expression in NSCLC and its correlation with clinicopathological parameters and prognosis, determined by TMA-IHC. (*a1* and *a2*) Negative for DPP9 protein expression in normal tissues adjacent to non-cancerous tissue samples; (*b1* and *b2*) positive for DPP9 protein expression in squamous cell carcinoma tissues; (*c1* and *c2*) Positive for DPP9 protein expression in adenocarcinoma tissues. (*a1*, *b1* and *c1*) were ×40 magnification (bar = 500 μm), (*a2*, *b2* and *c2*) were ×400 magnification (bar = 50 μm). Positive DPP9 protein expression on cancerous cell cytoplasm was indicated by red arrows, and negative DPP9 protein expression on adjacent non-cancerous cells was indicated by green arrows; (*d* and *e*) Kaplan–Meier survival curves indicated that the protein expression of DPP9 and TNM stage were significantly associated with the overall survival rate of NSCLC patients.

#### Analysis of DPP9 expression in NSCLC patients by TMA-IHC

We further evaluated the expression patterns and subcellular localizations of DPP9 protein in NSCLC tissues and non-tumor tissues by IHC analysis for 217 patients. Representative images of DPP9 staining are shown in Figure 2. Positive DPP9 staining was predominantly localized to the cellular membrane and cytoplasm in NSCLC tissues. The expression level of DPP9 protein in normal lung tissues (Figs. (1 and

2)*a1* and *2a2*) was clearly lower than that of squamous cell lung carcinoma (Figs. (1 and 2)*b1* and *2b2*) and adenocarcinoma tissues (Figs. (1 and 2)*c1* and *2c2*).

#### Association between DPP9 expression and clinicopathological parameters in NSCLC

The association between high DPP9 expression and clinicopathological variables of NSCLC patients ( $n = 217$ ) is

**Table 1.** Correlation of DPP9 expression in tumorous tissues with clinicopathologic characteristics in NSCLC patients

Clinicopathologic characteristics	n	DPP9		Pearson $\chi^2$	p
		Low or no expression	High expression		
Total	217	86 (39.63)	131 (60.37)		
Gender				3.762	0.052
Male	53	15 (28.30)	38 (71.70)		
Female	164	71 (43.29)	93 (56.71)		
Age at diagnosis (years)				1.498	0.221
$\leq 60$	71	24 (33.80)	47 (66.20)		
$> 60$	146	62 (42.47)	84 (57.53)		
Smoking				2.080	0.149
No smoking	131	57 (43.51)	74 (56.49)		
Smoking	86	29 (33.72)	57 (66.28)		
Histopathology Grading				3.289	0.193
Adenocarcinoma	33	16 (48.48)	17 (51.52)		
Squamous cell carcinoma	71	47 (66.20)	24 (33.80)		
Others <sup>a</sup>	35	23 (65.71)	12 (34.29)		
Differentiation				3.853	0.146
Low grade	29	11 (37.93)	18 (62.07)		
Middle grade	121	42 (34.71)	79 (65.29)		
High grade	67	33 (49.25)	34 (50.75)		
Primary tumor				1.795	0.408
T1	72	31 (43.06)	41 (56.94)		
T2	122	47 (38.52)	75 (61.48)		
T3+T4	19	5 (26.52)	14 (73.68)		
Unknown	4	3 (75.00)	1 (25.00)		
Lymph node metastasis				7.137	0.028 <sup>1</sup>
No regional lymph node metastasis	118	56 (47.46)	62 (52.54)		
Ipsilateral peribronchial metastasis	57	19 (33.33)	38 (66.67)		
Mediastinal metastasis	42	11 (26.19)	31 (73.81)		
Stage Grouping with TNM				6.451	0.040 <sup>1</sup>
Stage I	83	40 (48.19)	43 (51.81)		
Stage II	71	20 (28.17)	51 (71.83)		
Stage III+IV	59	23 (38.98)	36 (61.02)		
Unkown	4	3 (75.00)	1 (25.00)		

<sup>1</sup> $p < 0.05$  a, others, Adenosquamous carcinoma.

summarized in Table 1. A total of 131 (60.37%) patients showed high expression of DPP9, while 86 (39.63%) showed low or no expression of DPP9. High DPP9 expression was significantly associated with lymph node metastasis ( $p = 0.028$ ) and tumor node metastasis (TNM) stage ( $p = 0.040$ ). By contrast, no correlation ( $p > 0.05$  for all) was observed between DPP9 expression and other clinical parameters, such as sex, age at diagnosis, smoking, histopathology grading, differentiation and primary tumor (Table 1). Taken together, this shows that elevated DPP9 expression occurs alongside lymph node metastasis and poor TNM stage.

### Survival analysis

Findings from the univariate and multivariate analyses of prognostic variables for the 5-year survival rate of NSCLC are shown in Table 2. Univariate Cox regression analyses for all variables suggested that the overexpression of DPP9 (hazard ratio (HR) 1.639, 95% confidence interval (CI) 1.210–2.220,  $p = 0.001$ ) was a significant negative prognostic factor for 5-year OS in patients with NSCLC. Kaplan–Meier survival curves further confirmed that DPP9 protein expression was significantly associated with the OS of NSCLC patients, which was gradually reduced with increasing DPP9 expression (log-rank

**Table 2.** Univariate and multivariate analysis of prognostic factors of 5-year overall survival in NSCLC patients

Characteristic	Univariate analysis			Multivariate analysis		
	HR	<i>p</i>	95%CI	HR	<i>p</i>	95%CI
DPP9 expression	1.639	0.001 <sup>1</sup>	1.210–2.220	1.581	0.003 <sup>1</sup>	1.164–2.146
High vs. Low						
Gender	0.921	0.630	0.659–1.287			
Male vs. Female						
Age (years)	1.064	0.698	0.779–1.451			
≤60 vs. >60						
Smoking	0.875	0.388	0.647–1.185			
No smoking vs. smoking						
Histopathology Grading	0.874	0.186	0.716–1.067			
Ad vs. Sq vs. others						
Differentiation	1.142	0.262	0.906–1.440			
Low vs. middle vs. high grade						
Primary tumor	1.158	0.244	0.905–1.481			
T1 vs. T2 vs. T3+T4						
Lympho node metastasis	1.429	<0.001 <sup>1</sup>	1.194–1.710			
N0 vs. N1 vs. N2						
TNM stage	1.418	<0.001 <sup>1</sup>	1.189–1.691	1.429	<0.001 <sup>1</sup>	1.194–1.710
I vs. II vs. III+IV						

<sup>1</sup>*p* < 0.05 TNM stage contains N stage, therefore, N stage was not included in the multivariate analysis.  
Ad: Adenocarcinoma; Sq: Squamous cell carcinoma.

test, *p* < 0.001, Fig. 2d). The survival curve corresponding to DPP9 expression showed a good discrimination without too much overlap, indicating the success of the score standard for assessing DPP9 staining, and the reliability of DPP9 as a prognostic factor.

Moreover, the presence of lymph node metastasis (HR 1.429, 95% CI 1.194–1.710, *p* < 0.001), and advanced TNM stage (HR 1.418, 95% CI 1.189–1.691, *p* < 0.001) were significantly associated with the NSCLC patient survival. Kaplan–Meier survival curves revealed that patients with an early TNM stage had a significantly better prognosis than those with later stages (log-rank test, *p* < 0.001, Fig. 2e).

Finally, multivariate Cox regression analysis of the same set of NSCLC patients further demonstrated that DPP9 overexpression (HR 1.581, 95% CI 1.164–2.146, *p* = 0.003) is an independent prognostic factor for 5-year OS in patients with NSCLC. Advanced TNM stage (HR 1.429, 95% CI 1.194–1.710, *p* < 0.001) was also an independent prognostic marker for patient survival (Table 2).

#### Repression of DPP9 inhibits cell proliferation, migration and invasion *in vitro*

The A549 and H1299 cell lines showed high DPP9 expression. So the PGPH1/GFP/Neo vectors containing DPP9 shRNA-1 were transfected into these two cell lines. And we used G418 to establish the two stable DPP9 silencing cell lines. We first analyzed the effect of DPP9 on cell

proliferation. Compared with control cells, the CCK-8 assay found that knockdown of DPP9 by shDPP9 effectively inhibited proliferation ability in transfected cells at different time points (Fig. 3a). Next, we explored the role of DPP9 in the migration and invasion of A549 and H1299 cells. Migration assays showed that cell motility was dramatically reduced in shDPP9-transfected cells, compared with control cells. Similarly, the Matrigel invasion assay revealed that invasiveness was significantly suppressed in shDPP9-transfected cells (Fig. 3b). We noticed no significant change in DPP8 protein expression level while we silenced the DPP9. The results of the western blot analysis were shown in Supporting Information Figure 1a.

#### Overexpression of DPP9 in H1650 cell affects cell proliferation, migration and invasion in EMT markers and apoptosis-related proteins *in vitro*

We introduced a FoxQ1 cDNA expression vector into H1650 cell lines, where it indicated low DPP9 protein expression. Then we used G418 screening to establish the stable cell lines which overexpressed DPP9 protein in H1650 cell lines. Comparing the control cells, cells that overexpressed DPP9 protein in H1650 had higher levels of cell proliferation than the corresponding vector control and normal control cells at different time points (Supporting Information Fig. 1b). Next we explored the influence of DPP9 over expression for invasion and migration of H1650 cells. Invasion assay revealed that invasiveness was significantly elevated in shDPP9-transfected

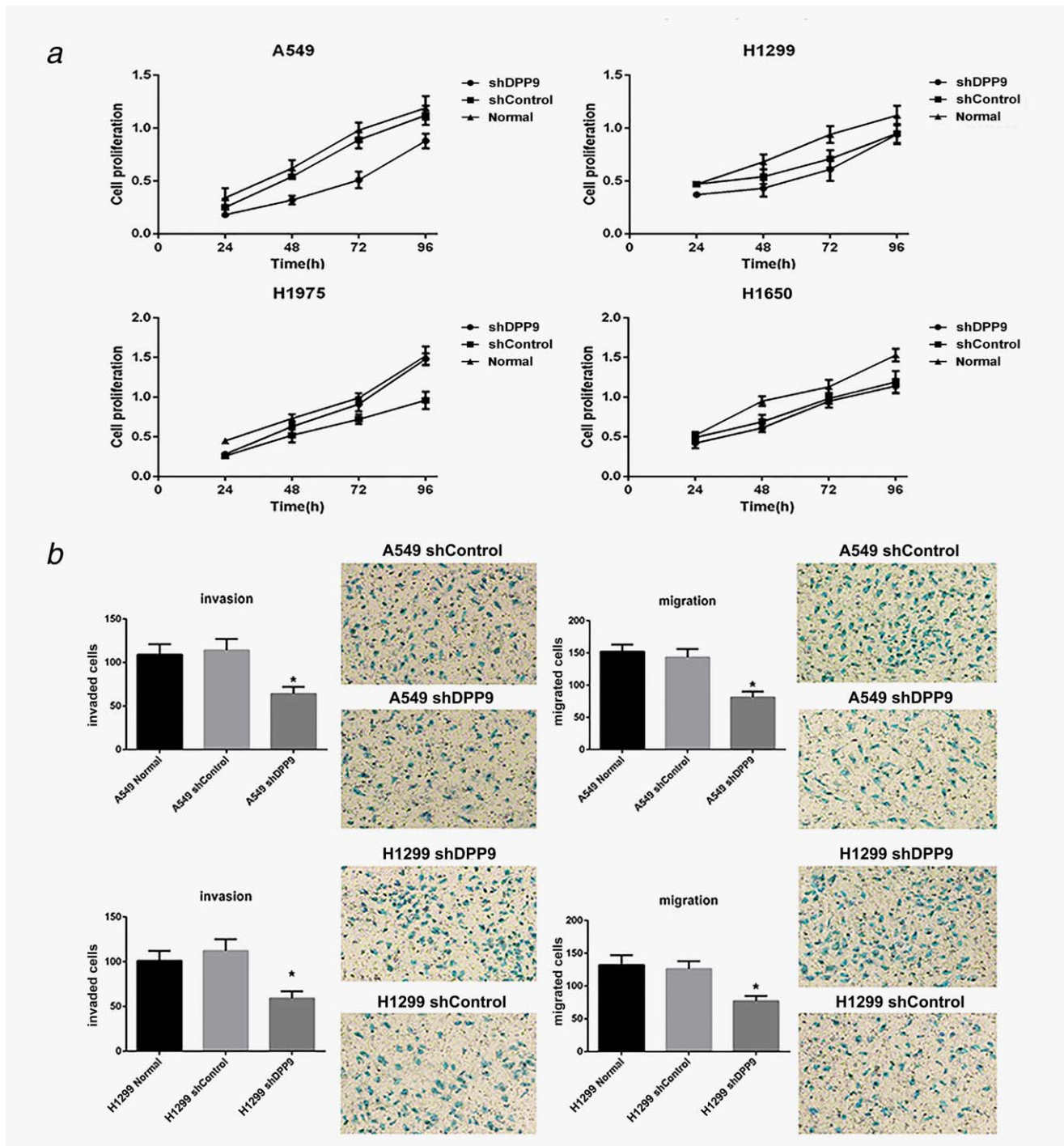


**Figure 3.** Effect of DPP9 in regulating NSCLC cells proliferation and motility *in vitro*. (a) CCK-8 assay indicated that knockdown of DPP9 by shDPP9 could effectively inhibit tumorigenic ability in A549, H1299, H1975 and H1650 cells; (b) Transwell assay (representative micrographs were presented) showed that cell migration and invasion in shDPP9-transfected cells compared with control cells. Data are presented as means  $\pm$  SD;  $n = 5-8$ /group. \*  $p < 0.05$ , \*\*  $p < 0.01$ .

cells, similarly the migration assay revealed that the cell motility was significantly accelerated in shDPP9-transfected cells (Supporting Information Fig. 1c). These data suggested that DPP9 regulates NSCLC cell proliferation and motility. Then we examined EMT-marker for H1650-OE transfection, where the protein levels of E-cadherin and MUC1 were significantly decreased,

while Vimentin, S100A4 and SNAIL were markedly increased in cells compared with shControl cells *in vitro* (Supporting Information Figs. D and F). We next examined apoptosis-related proteins, significantly decreased expression of p53, BAX and APAF1 were detected in H1650-OE transfected cells compared with shControl cells (Supporting Information Figs. E and G).

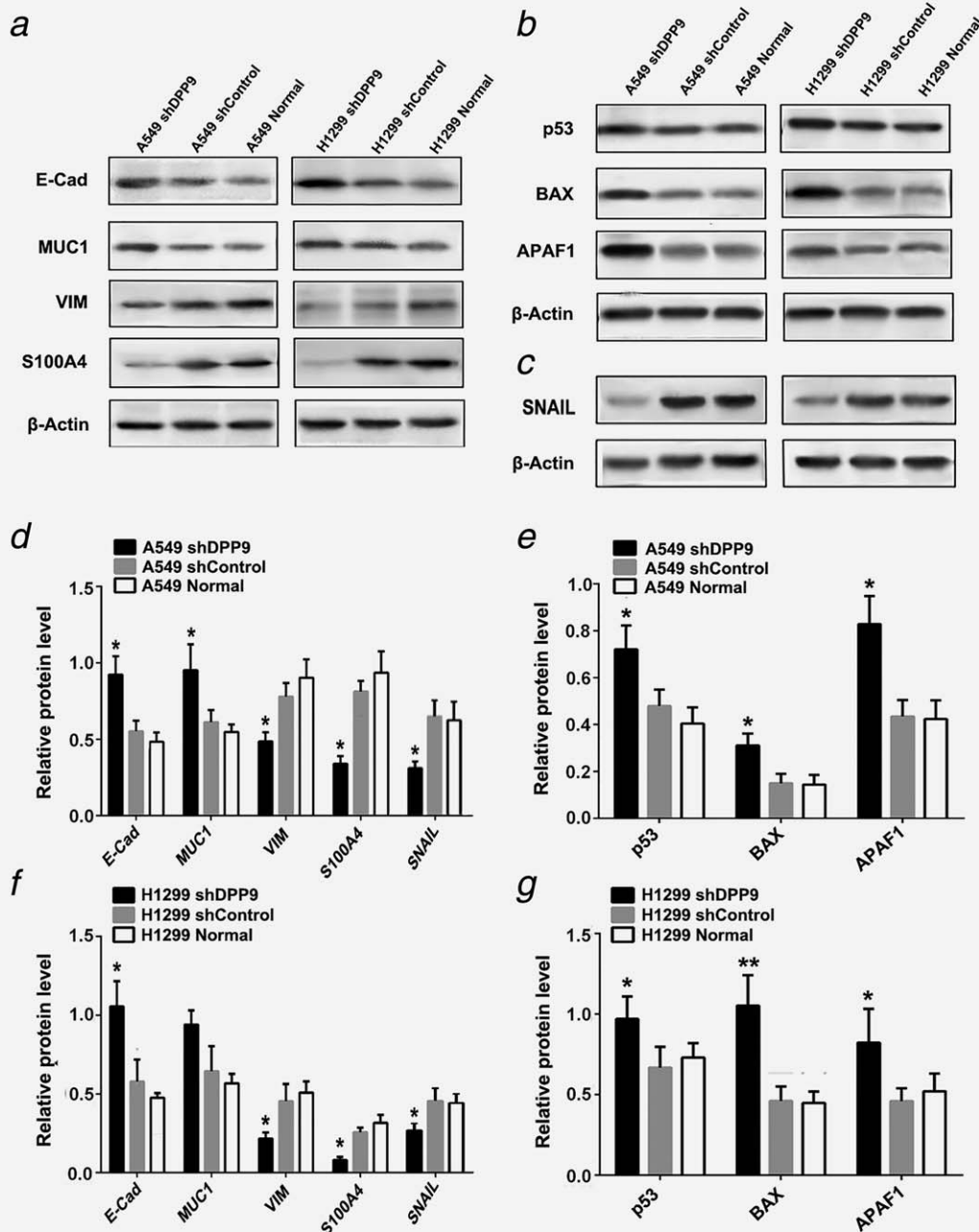


**Figure 4.** Repression of DPP9 in regulating EMT markers and apoptosis-related proteins. (a, c, d and f) Western blot analysis of EMT markers (E-Cad, MUC1, VIM, S100A4 and SNAIL) expression in DPP9 silenced cells. (b, e and g). Western blot analysis of apoptosis-related proteins (p53, BAX and APAF1) expression in DPP9 silenced cells. The loading control was  $\beta$ -actin. Data are presented as means  $\pm$  SD;  $n = 5-8$ /group. \*  $p < 0.05$ , \*\*  $p < 0.01$ .

#### Repression of DPP9 regulates EMT markers and apoptosis-related proteins *in vitro* and *in vivo*

We further analyzed the effects of DPP9 on EMT markers and apoptosis-related proteins. Following shDPP9 transfection, the protein levels of E-cadherin and MUC1 were significantly increased, while vimentin, S100A4 and SNAIL were markedly decreased in cells compared with control cells and normal cells *in vitro* (Figs. 4a, 4c, 4d and 4f), except the

expression of MUC1 in H1299 cells. We next examined apoptosis-related proteins. Significantly increased expression of p53, BAX, and APAF1 was detected in shDPP9-transfected cells compared with control cells and normal cells (Figs. 4b, 4e and 4g).

We also investigated metastasis- and apoptosis-associated protein expression *in vivo*. Western blot analysis of tumor xenograft tissues was consistent with the abovementioned

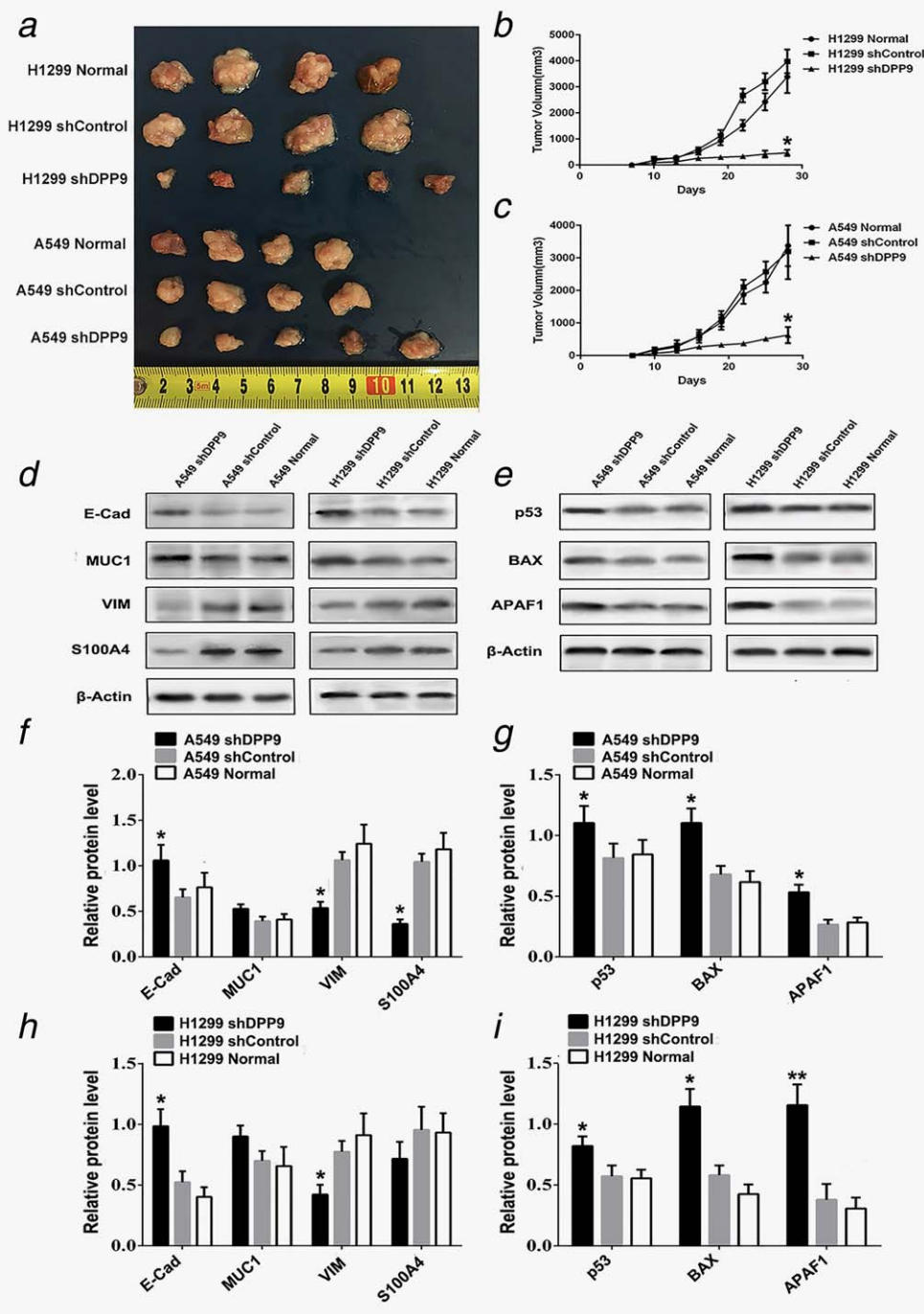


**Figure 5.** Repression of DPP9 in regulating tumorigenicity of NSCLC, expressions of EMT markers and apoptosis-related proteins in tumor xenograft model. (a) Photo of tumors in shDPP9-transfected cells compared with normal and control cells in nude mice; (b and c) The tumor growth curves in shDPP9-transfected cells compared with corresponding control and normal control mice. (d) EMT markers; (e) Apoptosis markers; (f) Graphical representation of EMT marker for A549 shDPP9. (g) Graphical representation of Apoptosis marker for A549 shDPP9. (h) Graphical representation of EMT marker for H1299 shDPP9. (i) Graphical representation of Apoptosis marker for H1299 shDPP9. Data are presented as means  $\pm$  SD;  $n = 5-8$ /group. \*  $p < 0.05$ , \*\*  $p < 0.01$ .

results (Figs. 5d and 5e). Thus, the expression of E-cadherin, MUC1, p53, BAX and APAF1 were increased (Figs. 1f), while that of vimentin, and S100A4 was decreased in tumors stably silenced for DPP9 expression.

**Repression of DPP9 inhibits tumorigenicity of NSCLC cells *in vivo***

To further explore the function of DPP9 in NSCLC *in vivo*, Normal, shControl and shDPP9 H1299 and A549 cells were

injected subcutaneously into BALB/c athymic nude mice. And tumorigenicity was monitored. Repression of DPP9 resulted in the dramatic retardation of tumor growth *in vivo*. The tumor volume in DPP9 knockdown mice was clearly reduced compared with normal and control groups (Fig. 5a). Growth curves also showed that the tumor volume in DPP9-silenced groups was much lower than that in corresponding control and normal control mice (Figs. 5b and 5c). Taken together, these results revealed that DPP9 showed a preliminary oncogenetic function in the development of NSCLC.

## Discussion

DPP9 belongs to the *S9b* enzyme family (also known as the *DPP4* gene family),<sup>18</sup> and its biological function in human cancer is largely unknown. In this study, we found that DPP9 expression was significantly increased in NSCLC tissues compared with adjacent non-tumor tissues, and correlated with a poor OS rate in NSCLC patients. Furthermore, loss-of-function analyses revealed that DPP9 promoted the proliferation, migration, and invasion of NSCLC cells. These findings highlight the potential tumor promotion role of DPP9 in NSCLC.

The malignant transformation of NSCLC is a complicated multifactor, multistep process involving multiple genes.<sup>19</sup> The predominant reason for carcinogenesis can be attributed to the down-regulation of tumor suppressor genes and the up-regulation of oncogenes or cancer-promoting genes.<sup>20</sup> The DPP4 enzyme family is expressed and is found in all normal human adult and neonatal tissues.<sup>21–23</sup>

DPP9 and DPP4 share a high sequence homology, and possess a very similar tertiary structure and functional activity.<sup>17</sup> However, the intracellular functions of DPP9 are less clear. DPP9 has two forms and a broad tissue distribution.<sup>12</sup> Waumans *et al.*<sup>24</sup> reported that DPP9 expression was relatively low in mouse monocytes and macrophages. Moreover, the inhibition of DPP9 attenuated macrophage activation by significantly reducing the secretion of interleukin-6.<sup>16</sup> Another recent study showed that DPP9 enzymatic activity regulates metabolic pathways in the neonatal liver and gut, and is essential for neonatal development.<sup>25</sup>

DPP9 siRNA knockdown or enzyme inhibition inhibits tumor cell adhesion and migration, possibly through down-regulating phosphorylation of focal adhesion kinase and paxillin.<sup>26</sup> DPP9 influences interferon  $\gamma$  secretion and antigen presentation on major histocompatibility complex class I molecules, suggesting a novel role for DPP9 in antigen maturation and presentation.<sup>27</sup> In 2013, Wilson and colleagues published the first proteomic screen for natural DPP8 and DPP9 substrate discovery. Utilizing N-terminal TAILS, they were able to identify 29 substrate candidates (23 for DPP8 and 17 for DPP9) and confirmed cleavage of 9/14 substrates. The antigenic peptide renal ubiquitin 1 was the first natural substrate of DPP9 to be identified.<sup>27</sup> In another study conducted by Wilson *et al.* reported that, adenylate kinase 2 and calreticulin were identified and validated as substrates of both

DPP8 and DPP9, where Adenylate kinase 2 plays an important role in maintaining cellular energy homeostasis.

DPP9 has also been studied in several types of human cancer, and has a diverse range of biological effects on transformed cells. For instance, DPP9 expression is significantly increased in testicular cancer,<sup>11</sup> and DPP9 enzymatic activity is associated with a malignant behavior in human astrocytic tumors.<sup>13</sup> Additionally, the inhibition of intracellular DPP9 enhances the anti-leukemic activity of parthenolide,<sup>28</sup> while DPP9 may also act as a survival factor for cells from the Ewing's sarcoma family of tumors cells and protect them against cell death induced by endogenous neuropeptide Y.<sup>29</sup> On the other hand, DPP9 overexpression was reported to inhibit phosphoinositide 3-kinase/Akt signaling in an epidermal growth factor receptor-dependent manner, attenuating cell proliferation and promoting apoptosis in human hepatoma cells.<sup>30</sup> Therefore, the pro- or anti-tumor activity of DPP9 may depend on the cell type and the molecular context within the tumor microenvironment.

In our study, we observed that the knockdown of DPP9 expression inhibited cell proliferation, migration, and invasion *in vitro*, and inhibited the tumorigenicity of NSCLC cells *in vivo*. Furthermore, high DPP9 expression was significantly associated with lymph node metastasis and TNM stage. Multivariate analysis showed that DPP9 overexpression was an independent prognostic factor for poor 5-year overall survival in NSCLC patients. All these results support a tumor promotion role for DPP9, which is consistent with most previous studies, in the initiation and progression of NSCLC.

We also explored the downstream effectors that mediate the regulation of proliferation and metastasis by DPP9. The developmental program of epithelial-mesenchymal transition (EMT) has been confirmed to play a pivotal role in promoting metastasis in epithelium-derived carcinoma.<sup>31–35</sup> During the oncogenesis process, epithelial tumor cells underwent EMT and displayed an enhanced invasive and metastatic capacity.<sup>36,37</sup> In our study, the expression of E-cadherin and vimentin (epithelial markers) were significantly increased in shDPP9-transfected cells. Loss of E-cadherin is considered to be a critical event in EMT<sup>38</sup> that regulates cellular dimensions and cell shape.<sup>39</sup> The loss of functional E-cadherin is thus a hallmark of EMT.<sup>40,41</sup> Additionally, we found that the knockdown of DPP9 also reduced the expression of MUC1 and S100A4 (mesenchymal markers). The expression of these proteins were previously shown to correlate with poor survival in NSCLC patients,<sup>42,43</sup> while their knockdown suppresses tumor growth and metastasis in NSCLC cells.<sup>43,44</sup> Our investigation of apoptosis-related protein expression detected a significantly increased expression of p53, BAX, and APAF1, which all play a crucial role in cell apoptosis.<sup>45,46</sup>

Higher DPP9 expression in NSCLC tissues were significantly associated with inferior survival independently of conventional prognostic factors, which further confirmed that DPP9 up-regulation promotes NSCLC development. Survival outcome varies among NSCLC patients, even within groups

that present with the same stage at the time of diagnosis and who were treated in similar strategies.<sup>5,47</sup> Therefore, there is a need to develop accurate individual prognostic factors. In recent years, emerging novel molecular prognostic and predictive markers have been reported and showed promising results in NSCLC patients, such as estrogen receptor  $\beta$ ,<sup>48</sup> regulatory T cells<sup>49</sup> and tumor-associated macrophage infiltration.<sup>50</sup> In this study, we found that the up-regulation of DPP9 was able to predict poor prognosis of NSCLC patients. To the best of our knowledge, this is the first study to evaluate the clinical value of DPP9 as a prognostic marker in human cancers.

Repression of DPP9 inhibits cell proliferation, migration and invasion *in vitro*, which suggests that DPP9 regulates NSCLC cell proliferation and motility, likewise repression of DPP9 inhibits the tumorigenicity of NSCLC cells *in vivo*. Taken together, these results revealed that DPP9 plays a tumor-promoting role in the development of NSCLC.

Overall, our study suggests that DPP9 plays a potential tumor promotion role in NSCLC, for during our study we

observed that in CCK-8 assays the knockdown of DPP9 by shDPP9 effectively inhibited the proliferation ability in transfected cells at different time points, these data suggested that DPP9 regulates NSCLC cell proliferation and motility *in vitro* and we also observed that repression of DPP9 resulted in the dramatic retardation of tumor initiation and growth *in vivo*. The tumor volume in DPP9 knockdown mice was clearly reduced compared with normal and control groups. Growth curves also showed that the tumor volume in DPP9-silenced groups was much lower than that in corresponding control and normal control mice. Since DPP9 knockdown was able to suppress tumorigenesis and metastasis in NSCLC cells, this could be a vigorous therapeutic strategy for future NSCLC treatment.

### Acknowledgement

We thank the clinical biobank members in Affiliated Hospital of Nantong University.

### References

- Jemal A, Bray F, Center MM, et al. Global cancer statistics. *CA Cancer J Clin* 2011;61:69–90.
- Owonikoko TK, Ragin CC, Belani CP, et al. Lung cancer in elderly patients: an analysis of the surveillance, epidemiology, and end results database. *J Clin Oncol* 2007;25:5570–7.
- Sher T, Dy GK, Adjei AA. Small cell lung cancer. *Mayo Clin Proc* 2008;83:355–67.
- Minguet J, Smith KH, Bramlage P. Targeted therapies for treatment of non-small cell lung cancer—Recent advances and future perspectives. *Int J Cancer* 2016;138:2549–61.
- Molina JR, Yang P, Cassivi SD, et al. Non-small cell lung cancer: epidemiology, risk factors, treatment, and survivorship. *Mayo Clin Proc* 2008;83:584–94.
- Gall MG, Chen Y, de Ribeiro AJV, et al. Targeted inactivation of dipeptidyl peptidase 9 enzymatic activity causes mouse neonate lethality. *PLoS One* 2013;8:e78378.
- Gonzalez-Gronow M, Kaczowka S, Gawdi G, et al. Dipeptidyl peptidase IV (DPP IV/CD26) is a cell-surface plasminogen receptor. *Front Biosci* 2008;13:1610–8.
- Wilson CH, Zhang HE, Gorrell MD, et al. Dipeptidyl peptidase 9 substrates and their discovery: current progress and the application of mass spectrometry-based approaches. *Biol Chem* 2016;397:837–56.
- Zhang H, Maqsudi S, Rainczuk A, et al. Identification of novel dipeptidyl peptidase 9 substrates by two-dimensional differential in-gel electrophoresis. *Febs J* 2015;282:3737–57.
- Yu DM, Wang XM, McCaughan GW, et al. Extraenzymatic functions of the dipeptidyl peptidase IV-related proteins DP8 and DP9 in cell adhesion, migration and apoptosis. *Febs J* 2006;273:2447–60.
- Yu DM, Ajami K, Gall MG, et al. The *in vivo* expression of dipeptidyl peptidases 8 and 9. *J Histochem Cytochem* 2009;57:1025–40.
- Ajami K, Abbott CA, McCaughan GW, et al. Dipeptidyl peptidase 9 has two forms, a broad tissue distribution, cytoplasmic localization and DP9-like peptidase activity. *Biochim Biophys Acta* 2004;1679:18–28.
- Stremenova J, Krepela E, Mares V, et al. Expression and enzymatic activity of dipeptidyl peptidase-IV in human astrocytic tumours are associated with tumour grade. *Int J Oncol* 2007;31:785–92.
- Ajami K, Pitman MR, Wilson CH, et al. Stromal cell-derived factors alpha and inflammatory protein-10 and interferon-inducible T cell chemoattractant are novel substrates of dipeptidyl peptidase 8. *FEBS Lett* 2008;582:819–25.
- Maes MB, Dubois V, Brandt I, et al. Dipeptidyl peptidase 8/9-like activity in human leukocytes. *J Leukoc Biol* 2007;81:1252–7.
- Matheussen V, Waumans Y, Martinet W, et al. Dipeptidyl peptidases in atherosclerosis: expression and role in macrophage differentiation, activation and apoptosis. *Basic Res Cardiol* 2013;108:350.
- Zhai X, Xu L, Zhang S, et al. High expression levels of MAGE-A9 are correlated with unfavorable survival in lung adenocarcinoma. *Oncotarget* 2016;7:4871–81.
- Liu J, Huan Y, Li C, et al. Establishment of a selective evaluation method for DPP4 inhibitors based on recombinant human DPP8 and DPP9 proteins. *Acta Pharm Sin B* 2014;4:135–40.
- Xie D, Lan L, Huang K, et al. Association of p53/p21 expression and cigarette smoking with tumor progression and poor prognosis in non-small cell lung cancer patients. *Oncol Rep* 2014;32:2517–26.
- Lee EY, Muller WJ. Oncogenes and tumor suppressor genes. *Cold Spring Harb Perspect Biol* 2010;2:a003236.
- Abbott CA, Yu DM, Woollatt E, et al. Cloning, expression and chromosomal localization of a novel human dipeptidyl peptidase (DPP) IV homolog, DPP8. *Eur J Biochem* 2000;267:6140–50.
- Dubois V, Van Ginneken C, De Cock H, et al. Enzyme activity and immunohistochemical localization of dipeptidyl peptidase 8 and 9 in male reproductive tissues. *J Histochem Cytochem* 2009;57:531–41.
- Yu DM, Yao TW, Chowdhury S, et al. The dipeptidyl peptidase IV family in cancer and cell biology. *Febs J* 2010;277:1126–44.
- Waumans Y, Vliegen G, Maes L, et al. The dipeptidyl peptidases 4, 8, and 9 in mouse monocytes and macrophages: DPP8/9 inhibition attenuates m1 macrophage activation in mice. *Inflammation* 2016;39:413–24.
- Chen Y, Gall MG, Zhang H, et al. Dipeptidyl peptidase 9 enzymatic activity influences the expression of neonatal metabolic genes. *Exp Cell Res* 2016;342:72–82.
- Zhang H, Chen Y, Wadham C, et al. Dipeptidyl peptidase 9 subcellular localization and a role in cell adhesion involving focal adhesion kinase and paxillin. *Biochim Biophys Acta* 2015;1853:470–80.
- Geiss-Friedlander R, Parmentier N, Möller U, et al. The cytoplasmic peptidase DPP9 is rate-limiting for degradation of proline-containing peptides. *J Biol Chem* 2009;284:27211–9.
- Spagnuolo PA, Hurren R, Gronda M, et al. Inhibition of intracellular dipeptidyl peptidases 8 and 9 enhances parthenolide's anti-leukemic activity. *Leukemia* 2013;27:1236–44.
- Lu C, Tilan JU, Everhart L, et al. Dipeptidyl peptidases as survival factors in Ewing sarcoma family of tumors: implications for tumor biology and therapy. *J Biol Chem* 2011;286:27494–505.
- Yao TW, Kim WS, Yu DM, et al. A novel role of dipeptidyl peptidase 9 in epidermal growth factor signaling. *Mol Cancer Res* 2011;9:948–59.
- Tsai JH, Yang J. Epithelial-mesenchymal plasticity in carcinoma metastasis. *Genes Dev* 2013;27:2192–206.
- Lee KW, Kim JH, Han S, et al. Twist1 is an independent prognostic factor of esophageal squamous cell carcinoma and associated with its epithelial-mesenchymal transition. *Ann Surg Oncol* 2012;19:326–35.
- van Zijl F, Mall S, Machat G, et al. A human model of epithelial to mesenchymal transition to monitor drug efficacy in hepatocellular carcinoma progression. *Mol Cancer Ther* 2011;10:850–60.
- Yi ZY, Feng LJ, Xiang Z, et al. Vascular endothelial growth factor receptor-1 activation mediates

- epithelial to mesenchymal transition in hepatocellular carcinoma cells. *J Invest Surg* 2011;24:67–76.
35. Xu X, Zhu Y, Liang Z, et al. c-Met and CREB1 are involved in miR-433-mediated inhibition of the epithelial-mesenchymal transition in bladder cancer by regulating Akt/GSK-3beta/Snail signaling. *Cell Death Dis* 2016;7:e2088.
  36. Kalluri R, Weinberg RA. The basics of epithelial-mesenchymal transition. *J Clin Invest* 2009;119:1420–8.
  37. Miettinen PJ, Ebner R, Lopez AR, et al. TGF-beta induced transdifferentiation of mammary epithelial cells to mesenchymal cells: involvement of type I receptors. *J Cell Biol* 1994;127:2021–36.
  38. Qiao Y, Jiang X, Lee ST, et al. FOXQ1 regulates epithelial-mesenchymal transition in human cancers. *Cancer Res* 2011;71:3076–86.
  39. van Roy F, Berx G. The cell-cell adhesion molecule E-cadherin. *Cell Mol Life Sci* 2008;65:3756–88.
  40. Aclouque H, Adams MS, Fishwick K, et al. Epithelial-mesenchymal transitions: the importance of changing cell state in development and disease. *J Clin Invest* 2009;119:1438–49.
  41. Peinado H, Olmeda D, Cano A. Snail, Zeb and bHLH factors in tumour progression: an alliance against the epithelial phenotype. *Nat Rev Cancer* 2007;7:415–28.
  42. Guddo F, Giatromanolaki A, Koukourakis ML, et al. MUC1 (episialin) expression in non-small cell lung cancer is independent of EGFR and c-erbB-2 expression and correlates with poor survival in node positive patients. *J Clin Pathol* 1998;51:667–71.
  43. Stewart RL, Carpenter BL, West DS, et al. S100A4 drives non-small cell lung cancer invasion, associates with poor prognosis, and is effectively targeted by the FDA-approved anti-helminthic agent niclosamide. *Oncotarget* 2016;7:34630–42.
  44. Gao J, McConnell MJ, Yu B, et al. MUC1 is a downstream target of STAT3 and regulates lung cancer cell survival and invasion. *Int J Oncol* 2009;35:337–45.
  45. Hu Z, Zeng Q, Zhang B, et al. Promotion of p53 expression and reactive oxidative stress production is involved in zerumbone-induced cisplatin sensitization of non-small cell lung cancer cells. *Biochimie* 2014;107Pt B:257–62.
  46. Kannan K, Kaminski N, Rechavi G, et al. DNA microarray analysis of genes involved in p53 mediated apoptosis: activation of Apaf-1. *Oncogene* 2001;20:3449–55.
  47. Wouters MW, Siesling S, Jansen-Landheer ML, et al. Variation in treatment and outcome in patients with non-small cell lung cancer by region, hospital type and volume in the Netherlands. *Eur J Surg Oncol* 2010;36:S83–92.
  48. Ma L, Zhan P, Liu Y, et al. Prognostic value of the expression of estrogen receptor beta in patients with non-small cell lung cancer: a meta-analysis. *Transl Lung Cancer Res* 2016;5:202–7.
  49. Zhao S, Jiang T, Zhang L, et al. Clinicopathological and prognostic significance of regulatory T cells in patients with non-small cell lung cancer: A systematic review with meta-analysis. *Oncotarget* 2016;7:36065–73.
  50. Mei J, Xiao Z, Guo C, et al. Prognostic impact of tumor-associated macrophage infiltration in non-small cell lung cancer: A systemic review and meta-analysis. *Oncotarget* 2016;7:34217–28